Indian Journal of Pure & Applied Physics
Vol. 58, February 2020, pp. 120-126

First principles investigation of electronic and magnetic - propertiess of double perovskites A_2NRuO_6 (A_2=Ba_2, BaLa; N=V, Cr and Fe)

Mohamed Musa Hasab-Elkhalig

Department of Physics, College of Science and Arts in Muthnib, Qassim University, Saudi Arabia

Received 16 October 2018; accepted 2 December 2019

The electronic and magnetic properties of double perovskites A_2NRuO_6 (A_2 = Ba_2, BaLa; N = V, Cr, Fe) have been investigated using the first-principles density-functional theory (DFT) within the generalized gradient approximation (GGA) and GGA+U schemes. All compounds of (A_2 = Ba^{2+}) and doped (A_2 = $Ba^{2+}La^{3+}$) crystallize in a cubic structure with (Fm-3m) space group. The GGA results of (A_2 = Ba^{2+}) predict half-metallic (HM), semiconductor and metallic character when (N = V, Cr, Fe), respectively which are completely stabilize at the HM nature within (A_2 = $Ba^{2+}La^{3+}$) compounds. By including the exchange-correlation energy in GGA+U scheme, all compounds show a HM property, except for Ba_2FeRuO_6 which appears as an insulating material. In addition, GGGA and GGA+U calculations of spin magnetic moments suggest a ferrimagnetic (FI) character for A_2NRuO_6 (N = V and Cr), switch to a ferromagnetic (FM) nature when N = Fe. It is found that the two ions of N^{3+}– Ru^{5+} (A_2 = Ba_2) and N^{3+}– Ru^{4+} (A_2 = BaLa) are governed by the antiferromagnetic interactions N^{3+} (3d)–O^{2-} (2p)–Ru^{5+}/Ru^{4+} (4d) in high/low spin magnetic moments states.

Keywords: Magnetic materials, Perovskites, Electronic properties, DFT, GGA + U schemes

1 Introduction

In ordered double perovskites symbolized as A_2NMO_6 with (A = alkaline-earth or rare-earth metal; N and M = transition-metals), the difference in ionic size and valence state between N and M are essential for controlling their main properties. During the last decades a large number of A_2NMO_6 have been extensively investigated due to their interesting properties, metallicity, half-metallicity (HM), semi-conducting, insulating as well as ferromagnetism (FM), anti-ferromagnetism (AF), ferrimagnetism (FI), which make them attractive candidates for spintronics applications[1], solid-state fuel cells devices[2], semiconductor technologies[3], etc. In HM compounds of A_2NMO_6, the conduction electrons have one of two possible spin-polarization (S_P) orientations, spin-up ($n_\uparrow$) or spin-down ($n_\downarrow$), to transfer. The relative S_P can be estimated by calculating the ratio of spin-density difference to the total spin-density at the Fermi level (E_F), $S_P = (n_\uparrow - n_\downarrow)/(n_\uparrow + n_\downarrow)$. S_P lies in the range ($-1 \leq S_P \leq +1$) thus, (S_P = 0) for un-polarized electrons in semiconductors and insulators, whereas full-polarization in spin-up (S_P = +1) or spin-down (S_P = – 1) materializes in HM double perovskites[4-6]. Therefore, HM double perovskites have attracted special attention in many applied and fundamental fields of solid-state physics, materials science, materials engineering and materials technology. As a result, various chemical and physical properties have been studied in these compounds, for example, HM accompanied by a FI state have detected in a few Sr-based compounds[4-6] (Sr_2CrMoO_6), (Sr_2CrWO_6) and (Sr_2FeMoO_6). Based on their density of states (DOS) near E_F, HM double perovskite are characterized by the coexistence of metallic behavior in one electron spin channel of DOS and insulating behavior in the other channel. This nature often associates with the colossal magnetoresistance (MR) phenomenon that has been discovered in a few double perovskites, such as (Sr_2MMoO_6) with (M = Cr)[4] and (M = Fe)[7].

Furthermore, many theoretical and experimental studies have been devoted to the changing of metallic and magnetic ions on N and M sites to modify the structural, electronic, magnetic and other properties of A_2NMO_6. These studies intended for optimizing the magnetic properties of double perovskites in order to be useful for many applications in magneto-electronic devices such as magnetic storage systems, spin valves and spin polarization sources for spintronics devices. Along this way, the important aspect is to obtain sufficiently high Curie-temperature (T_C) and 100 % S_P, such as (T_C = 635 K) and HM in (Sr_2CrReO_6)[8], to allow for the operation of potential devices at room temperature (RT). The increase of T_C in Sr_2FeMoO_6

E-mail: 141261@qu.com.sa

was reported to be a result of the electron-doping via the partially substitution of Sr^{2+} sites by La^{3+} ions ($Sr_{2-x}La_xFeMoO_6$)[9]. With respect to MR, the large low-field MR effect has been established in (Sr_2CrWO_6)[5] and (Sr_2FeMoO_6)[6,7] as well as in doped compounds, such ($Sr_{2-x}La_xFeReO_6$)[10] and ($A_{2-x}B_x$ $FeMoO_6$) with (A = Sr, Ba; B = Sr, Mg)[11,12].

In this paper, first-principles calculations are carried out using the generalized gradient approximation (GGA) and (GGA+U) schemes to investigate the structural, electronic and magnetic properties of double perovskites (A_2NRuO_6) where (A_2 = Ba_2, BaLa; N = V, Cr, Fe). Moreover, the effects of 1:1 electron-doping on A^{2+}-site, N-site substitution and exchange-correlation (GGA+U) on these properties are discussed in detail. To the best of our knowledge, there are no previous experimental or theoretical reports on (A_2NRuO_6) compounds, so, this is the first time to investigate this series in detailed. The structural calculations showed that all compounds have a cubic structure (Fm-3m).

2 Computational Method and Calculation Details

Spin-polarized density functional theory (DFT) calculations were performed with the full potential linear muffin-tin orbital (FP-LMTO) using atomic plane-wave (APLW) method[13] as implemented in (LMTART) package[14,15]. The exchange-correlation was treated in the Perdew-Wang 1991 (PW91) version of GGA[13-15]. In addition, the electronic correlation effect (GGA+U) in N (3d) and Ru (4d) ions was considered[14] via the option of on-site coulomb repulsion (U) and exchange energy (J). (U = 4.0 eV, J = 0.89 eV) for N (3d) states and (U = 1.0 eV, J = 0.89 eV) for Ru (4d) states[4,16] were applied. The electronic configurations of atoms in (A_2NRuO_6) are Ba: [Xe] $6s^2$, La: [Xe] $5d^1$ $6s^2$, V: [Ar] $3d^3$ $4s^2$, Cr: [Ar] $3d^5$ $4s^1$, Fe: [Ar] $3d^6$ $4s^2$, Ru: [Kr] $4d^7$ $5s^1$, and O: [He] $2s^2$ $2p^4$. Therefore, core electrons were treated fully relativistically, whereas a scalar relativistic approximation was used for the valence electrons in Ba (6s), La (6s), N (3d 4s), Ru (4d 5s) and O (2p). A (6×6×6) *k*- mesh with 120 points in the irreducible part of the Brillouin zone (BZ) was taken into account, which is found to be well converged. To correctly describe the PLWs inside atoms, the spherical harmonics were expanded as (l_{max} = 6.0) for all LMTOs. Self-consistency (SCF) was assumed for a total energy convergence of less than (0.01 meV). BZ integration in the SCF iterations was performed over double kappa (κ = 2) for LMTO basis.

3 Results and Discussion

3.1 Structural properties

Among oxides, double perovskites possess very flexible crystal structure (A_2NMO_6), where A, M and N sites can be varied leading to a large number of compounds. Most double perovskites are distorted from the cubic structure; three factors are responsible for this distortion; size effect, deviations from ideal composition and Jahn-Teller effect. For size effect, according to the ionic radii, the tolerance factor (TF) allows to estimate the degree of distortion in A_2NMO_6, $TF = (\langle r_A \rangle + r_O)/\sqrt{2}(\langle r_{N,M} \rangle + r_O)$, where, $\langle r_A \rangle$, $\langle r_{N,M} \rangle$ and $\langle r_O \rangle$ are the average ionic radii of A^{2+}, N^{3+}–M^{5+} and O^{2-}, respectively. Accordingly, ideal cubic double perovskites have ($t \approx 1.00$); there is no tilting in NO_6 and MO_6 octahedra in order to fill the space. Many previous studies have shown that when ($0.99 < t < 1.05$) the double perovskites crystallize in cubic structure[17,18]. In this study, for A_2NRuO_6, the effective ionic radii are r(Ba^{2+}) = 1.61 Å, r(La^{3+}) = 1.50 Å, r(V^{3+}) = 0.64 Å, r(Cr^{3+}) = 0.615 Å, r(Fe^{3+}) = 0.645 Å, r(Ru^{5+}) = 0.565 Å and r(O^{2-}) = 1.4 Å[18]. Therefore, the TF of A_2NRuO_6 compounds were calculated and found to be amid in the range of cubic structure, Table 1.

The structural properties have been calculated using the structure prediction diagnostic software (SPuDS)[17] that allows the formula A_2NMO_6 in a rock-salt cation ordering. Calculated results of TF, unit cell volume (V), lattice constants (a = b = c), oxygen position O (x), and average bond-distances and bond-angles were calculated and summarized in Tables 1 and 2. It is found that all compounds of A_2NRuO_6 crystallize in a cubic symmetry (space group Fm-3m; No. 225) with an ideal lattice constant (a ≈ 8.00 Å)[17,19]. Table 3 displays the atomic positions in cubic unit cell of A_2NRuO_6. As shown in Fig. 1, the results demonstrate that the crystals of A_2NRuO_6 did not deviate from the ideal structure, since there are (i) no displacement of N and Ru from the centers of NO_6

Table 1 – Structural properties for A_2NRuO_6 (A_2 = Ba_2, BaLa; N = V, Cr, Fe).

A_2NRuO_6	A_2VRuO_6		A_2CrRuO_6		A_2FeRuO_6	
A_2-sites	Ba_2	BaLa	Ba_2	BaLa	Ba_2	BaLa*
TF	1.0509	0.9999	1.0560	1.0047	1.0467	0.9959
V (Å^3)	499.403	505.685	492.262	498.484	505.470	511.803
a (Å)	7.9338	7.9670	7.8958	7.9290	7.9658	7.9990
O (x)	0.2520	0.2510	0.2508	0.2498	0.2530	0.2520

* $BaLaFeRuO_6$; cubic (a = 7.9730 Å; XRD) Ref. [20]

Table 2 – Bond distances and bond angles in A_2NRuO_6 (A_2 = Ba_2, BaLa; N = V, Cr, Fe).

A_2NRuO_6	A_2VRuO_6		A_2CrRuO_6		A_2FeRuO_6	
A_2-sites	Ba_2	BaLa	Ba_2	BaLa	Ba_2	BaLa
Bond distances						
La (8c)–O (24e) ×12 (Å)		2.8168		2.8033		2.8281
Ba (8c)–O (24e) ×12 (Å)	2.8051	2.8168	2.7916	2.8033	2.8165	2.8281
N (4a)–O (24e) ×6 (Å)	1.9995	1.9995	1.9805	1.9804	2.0155	2.0155
Ru (4b)–O (24e) ×6 (Å)	1.9675	1.9840	1.9675	1.9840	1.9675	1.9840
Bond angles						
O (24e)–N (4a)–O (24e) (º)	90.00	90.00	90.00	90.00	90.00	90.00
O (24e)–Ru (4b)–O (24e) (º)	90.00	90.00	90.00	90.00	90.00	90.00
N (4a)–O (24e)–Ru (4b) (º)	180.0	180.0	180.0	180.0	180.0	180.0

Table 3 – Atoms, multiplicity, Wyckoff, symmetry, positions and occupancy for A_2NRuO_6 (A_2 = Ba_2, BaLa; N = V, Cr, Fe). The values of oxygen coordinate O (x) have listed in Table 1.

Atom	Multiplicity	Wyckoff	Symmetry	Positions			Occupancy
				x	**y**	**z**	
Ba	8	c	-43m	¼	¼	¼	0.5
La	8	c	-43m	¼	¼	¼	0.5
N	4	a	m-3m	0	0	0	1.0
Ru	4	b	m-3m	½	½	½	1.0
O	24	e	4mm	x	0	0	1.0

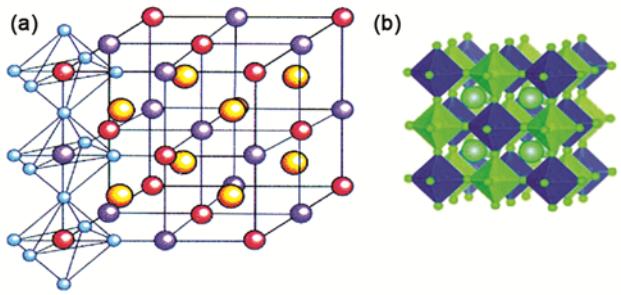

Fig. 1 – Crystal structure representation of cubic (space group Fm-3m) double perovskite (A_2NMO_6), where N^{3+} and M^{5+} atoms are arranged in a 1:1 rock-salt style. (a) The atomic positions of A (yellow), N (red) and M (violet), alternating N and M surrounded by oxygen (cyan) octahedral, and (b) corner-sharing view of octahedra NO_6 (blue) and MO_6 (green) where A cations (large green spheres) occupy every hole created by NO_6 and MO_6 octahedra.

and RuO_6 octahedra; (N–O ≈ Ru–O), (ii) no displacement of A_2 cations from the cavity centers, (iv) no distortion in NO_6 and RuO_6 octahedral cages (O–N– O = O–Ru–O = 90º) and (v) no tilt in NO_6 and RuO_6 octahedra (N–O–Ru = 180º).

3.2 Electronic properties

The total density of states (TDOS) and partial density of states (PDOS) of ordered double perovskites A_2NRuO_6 (A_2 = Ba_2, BaLa; N = V, Cr, Fe) were calculated using the GGA and GGA+U schemes. The electronic DFT-TDOS plots per unit cell for spin-up, upper curves (+TDOS) and spin-down, lower curves (–TDOS) are collectively presented in Fig. 2. The horizontal axis stands for the energy relative to the Fermi energy [E (eV)], thus, the E_F is situated at zero energy (dashed line; E_F = 0.0 eV). Figures 2 - 6 show the TDOS and PDOS behavior for these compounds, plotted between –8.0 eV and +8.0 eV, where the main electronic features occur. In order to realize the effects of electron doping, A_2 and N sites substitution, and the correlation energy, we discuss the electronic properties of A_2NRuO_6 in a general discussion. Figures 2 and 3 show the combined GGA and GGA+U curves of the TDOS of these compounds. From the GGA TDOSs around the E_F, it can see that the Ba_2NRuO_6 compounds show different electronic properties; HM (N = V), semiconducting (N = Cr) and metallic (N = Fe), which are completely transit to HM state when (A_2 = BaLa). When the correlated GGA+U method is applied, a clearly HM electronic nature is maintained in all A_2NRuO_6 compounds, except for the (N = Fe) compound with A_2 = Ba_2 which shows an electronic insulating state. The obtained results are in a good agreement with the pervious results[19-22]. Table 4 summarizes the results of the electronic energy-gap (E_g) and band-width (W) at the E_F, in spin-up and spin-down directions, for A_2NRuO_6 obtained from GGA and GGA+U calculations.

To gain deep insight into the partial contributions to the TDOS and various phenomena, the projected

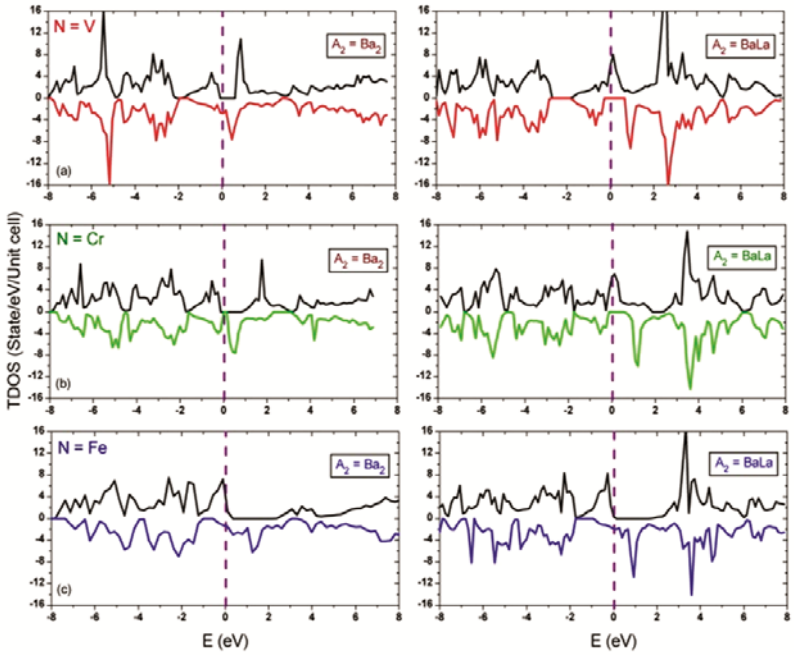

Fig. 2 – Spin-up and spin-down TDOS within GGA for A_2NRuO_6, $A_2 = Ba_2$ (left panels), A_2 = BaLa (right panels); (a) N = V, (b) N = Cr, and (c) N = Fe.

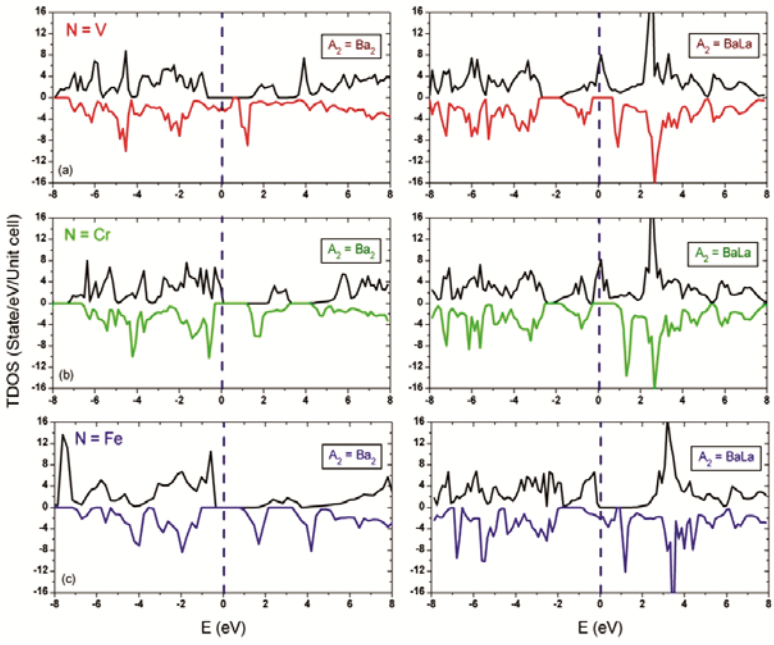

Fig. 3 – Spin-up and spin-down TDOS within GGA+U for A_2NRuO_6, $A_2 = Ba_2$ (left panels), A_2 = BaLa (right panels); (a) N = V, (b) N = Cr, and (c) N = Fe.

PDOS of M (3d), Ru (4d) and O (2p) are calculated using the GGA and GGA+U schemes. Figures 4, 5 and 6 shows the spin-up and spin-down PDOS of M (3d), Ru (4d) and O (2p) ions in six compounds. The PDOS of Ba and La ions are not given here since negligible interactions are observed between Ba and La ions and other ions in double perovskites A_2NRuO_6. From Fig. 4, we can see that the conduction band in spin-down between –1.5 and +1.5 eV almost come from the hybridization of V (3d) and O (2p) electrons in Ba_2VRuO_6. Switch to spin-up HM in $BaLaVRuO_6$ compound, here, the conduction band between –1.5 and +1.5 eV composes from the hybridization of Ru (4d) and O (2p) states. In

Table 4 – Spin-up (↑) and spin-down (↓) energy-gap (E_g) and band-width (W) from the TDOS (Figs 2 and 3) of A_2NRuO_6 (A_2 = Ba_2, BaLa; N = V, Cr, Fe), calculated using GGA and GGA+U schemes.

A_2NRuO_6		A_2VRuO_6		A_2CrRuO_6		A_2FeRuO_6	
A_2-sites		Ba_2	BaLa	Ba_2	BaLa	Ba_2	BaLa
GGA	E_g↑ (eV)	0.68	0.00	0.94	0.00	0.00	1.73
	E_g↓ (eV)	0.00	0.77	0.14	0.66	0.00	0.00
	W↑ (eV)	0.00	2.94	0.00	1.91	1.59	0.00
	W↓ (eV)	2.43	0.00	0.00	0.00	1.81	2.53
GGA+U	E_g↑ (eV)	1.89	0.00	2.24	0.00	1.82	1.61
	E_g↓ (eV)	0.00	0.94	1.48	1.34	1.82	0.00
	W↑ (eV)	0.00	2.40	0.00	0.93	0.00	0.00
	W↓ (eV)	1.98	0.00	0.00	0.00	0.00	1.73

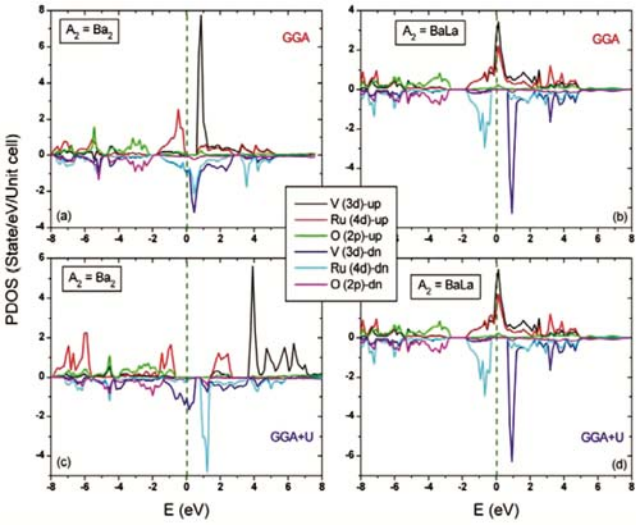

Fig. 4 – Spin-up and spin-down PDOS of V (3d), (c) Ru (4d) and (d) O (2p) states in A_2VRuO_6, A_2 = Ba_2 (left panels), A_2 = BaLa (right panels), calculated by (a)-(b) GGA, and (c)-(d) GGA+U schemes.

semiconductor Ba_2CrRuO_6, (Fig. 5), the spin-up and spin-down states of Cr (3d), Ru (4d) and O (2p) have significant contributions at the valence and conduction bands. Whereas, HM $BaLaCrRuO_6$ compound, the spin-up conduction band almost yields from the hybridizations of both Cr (3d)–O (2p) and Ru (4d) –O (2p) states between –1.5 and +1.5 eV. For the metallic compound Ba_2FeRuO_6, (Fig. 6), the spin-up and spin-down conduction band contain all the PDOS of Fe (3d), Ru (4d) and O (2p) states in GGA.

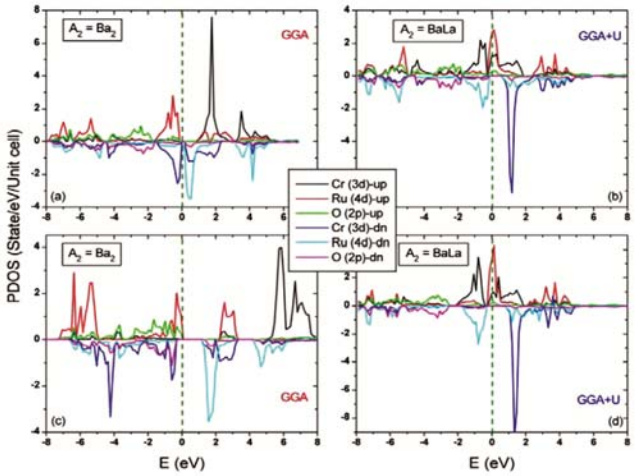

Fig. 5 – Spin-up and spin-down PDOS of Cr (3d), (c) Ru (4d) and (d) O (2p) states in A_2CrRuO_6, A_2 = Ba_2 (left panels), A_2 = BaLa (right panels), calculated by (a)-(b) GGA, and (c)-(d) GGA+U schemes.

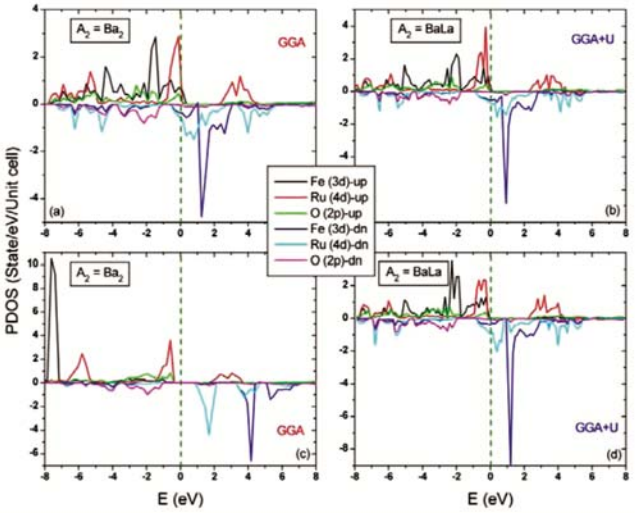

Fig. 6 – Spin-up and spin-down PDOS of Fe (3d), (c) Ru (4d) and (d) O (2p) states in A_2FeRuO_6, A_2 = Ba_2 (left panels), A_2 = BaLa (right panels), calculated by (a)-(b) GGA, and (c)-(d) GGA+U schemes.

While, the spin-down HM in $BaLaFeRuO_6$ compound, the conduction band come from the hybridization of Fe (3d) and O (2p) states.

3.3 Magnetic properties

To study the magnetic properties of double perovskites A_2NRuO_6 (A_2 = Ba_2, BaLa; N = V, Cr, Fe), the spin-polarized DFT calculations using the GGA and GGA+U schemes were carried out. The results of these calculations reveal that the (N = V) and (N = Cr) compounds possess ferrimagnetic (FI) nature within two schemes, while the (N = Fe) compounds possess ferromagnetic (FM) nature. The

Table 5 – Calculated spin magnetic moments per unit cell (in μ_B unit) for A_2NRuO_6 (A_2 = Ba_2, BaLa; N = V, Cr, Fe) by GGA and GGA+U schemes.

A_2NRuO_6		A_2VRuO_6		A_2CrRuO_6		A_2FeRuO_6	
A_2-sites		Ba_2	BaLa	Ba_2	BaLa	Ba_2	BaLa
GGA	Ba_2	0.042	-0.004	0.056	-0.029	0.062	0.055
	La	-	0.018	-	0.006	-	0.085
	N	-0.744	1.051	-2.123	2.040	4.213	3.729
	Ru	1.139	-0.818	1.447	-0.760	2.203	1.676
	O_6	0.488	-0.226	0.560	-0.318	0.720	0.579
GGA+U	Ba_2	0.074	-0.004	0.073	-0.005	0.047	0.048
	La	-	0.018	-	0.024	-	0.074
	N	-1.818	1.051	-2.034	2.301	4.502	3.923
	Ru	1.896	-0.818	2.034	-1.050	2.361	1.622
	O_6	0.732	-0.229	0.762	-0.290	0.714	0.528

major source of the magnetization in A_2NRuO_6 (A_2 = Ba_2) compounds is the N^{3+} (3d) and Ru^{5+} (4d) orbitals. Further analysis of the N^{3+} (3d) states shows that the 3d-t_{2g} orbitals are partially filled and the 3d-e_g orbitals are empty or filled by 2 electrons, as in (N = Fe). This reveals that the electronic configurations of N^{3+} (3d) ions are V^{3+} ($3d^2$; $t_{2g}^2\uparrow t_{2g}^0\downarrow e_g^0\uparrow e_g^0\downarrow$; S = 2/2), Cr^{3+} ($3d^3$; $t_{2g}^3\uparrow t_{2g}^0\downarrow e_g^0\uparrow e_g^0\downarrow$; S = 3/2), and Fe^{3+} ($3d^5$; $t_{2g}^3\uparrow t_{2g}^0\downarrow e_g^2\uparrow e_g^0\downarrow$; S = 5/2). As a result, the N^{3+} (3d) ions carry most of the spin magnetic moment, making them responsible for the FI and FM natures in three compounds of A_2NRuO_6. While in Ru^{5+} (4d) states, the 4d-t_{2g} orbitals are partially filled by three electrons and 4d-e_g orbitals are empty; Ru^{5+} ($4d^3$; $t_{2g}^3\uparrow t_{2g}^0\downarrow e_g^0\uparrow e_g^0\downarrow$; S = 3/2), thus, they hold a small spin magnetic moment that induced by the N (3d)–O (2p)–Ru (4d) hybridizations. In doped A_2NRuO_6 (A_2 = BaLa), since La has a devilant valance state La^{3+}, Ru (4d) modifies its valance state to Ru^{4+} ($4d^4$), hence, the extra electron occupies the spin-down of 4d-t_{2g} orbital; Ru^{4+} ($4d^4$; $t_{2g}^3\uparrow t_{2g}^1\downarrow e_g^0\uparrow e_g^0\downarrow$; S = 2/2).

The spin magnetic moments per unit cell of these compounds are calculated by two schemes and summarized in Table 5. It can be seen that the main contribution to the total magnetic moment of each compound comes from the energetic electrons of ions N (3d) and Ru (4d). The results of calculations also indicate that the electrons of O (2p) ions in all compounds can be polarized due to the hybridization between N (3d) and O (2p) states. Such hybridization induces AF coupling between N (3d) and Ru (4d) states in (N = V, Cr) compounds, and FM coupling in (N = Fe) compounds. In A_2NRuO_6 (N = V, Cr), the spin magnetic moments of N (3d) and Ru (4d) ions are almost different and antiparallel with a little contribution of O (2p) ions, which results in a non-zero net magnetic moment. Similar, behavior is observed in A_2NRuO_6 (N = Fe), except the spin magnetic moments of Fe (3d) and Ru (4d) are align in a parallel ordering, see Table 5. In all A_2NRuO_6 (A_2 = BaLa), the spin magnetic moment of Ru (4d) decreases, compared with the (A_2 = Ba_2) compounds, which is affected by the gaining of an extra doped-electron from La^{3+} ions. Therefore, the electronic configuration of Ru ions is modified to Ru^{4+} ($4d^4$) within the interaction N^{3+} (3d)–O^{2-} (2p)–Ru^{4+} (4d). In addition, the on-site Coulomb repulsion and exchange energy within (GGA+U) have a clear effect on spin magnetic moments. As shown in the bottom of Table 5, the spin magnetic moments of N (3d) and Ru (4d) are enhanced by employing GGA+U scheme.

4 Conclusions

In this study, the structural, electronic and magnetic properties of double perovskites A_2NRuO_6 (A_2 = Ba_2, BaLa; N = V, Cr, Fe) have been investigated using the FP-LMTO method. All compounds of A_2NRuO_6 have cubic crystal structure with space group Fm-3m. Spin-polarized electronic structure calculations based on GGA and GGA + U schemes were performed to investigate the electronic and magnetic properties of A_2NRuO_6. GGA and GGA+U schemes give different electronic properties; half-metallic (HM), semiconducting and metallic states are found within GGA if (A_2 = Ba_2; N = V, Cr, Fe), respectively, then all stabilize in a HM state when (A_2 = BaLa). GGA+U scheme produce a HM state in all these compounds, except for the Ba_2FeRuO_6, which shows an insulating behavior. The spin magnetic moment calculations reveal that the A_2NRuO_6 compounds have a ferrimagnetic (FI) nature if (N = V and Cr), switches to a ferromagnetic (FM) when (N =

Fe). The analysis demonstrates that the V^{3+}, Cr^{3+}, Fe^{3+} and Ru^{5+} ions are in high spin states due to the antiferromagnetic interaction N^{3+} (3d)–O^{2-} (2p)–Ru^{5+} (4d), whereas, Ru^{4+} ions are in low spin state in (A_2 = BaLa) case. Also, found that spin magnetic moments show strengthen with the La^{3+} substitution, on-site Coulomb repulsion and exchange energy on N (3d) and Ru (4d) electrons.

References

1 Kang J S, Han H, Lee B W, Olson C G, Han S W, Kim K H, Jeong J I, Park J H & Min B I, *Phys Rev B*, 64 (2001) 024429.

2 Wei T, Zhang Q, Huang Y H & Goodenough J B, *J Mater Chem*, 22 (2012) 225.

3 Kaloni T P, Kahaly M U, Cheng Y C & Schwingenschlögl U, *EPL*, 98 (2012) 67003.

4 Bonilla C M, Téllez D A L, Rodríguez J A, López E V & Rojas J R, *Physica B*, 398 (2007) 208.

5 Majewski P, Geprägs S, Boger A, Opel M, Erb A, Gross R, Vaitheeswaran G, Kanchana V, Delin A, Wilhelm F, Rogalev A & Alff L, *Phys Rev B*, 72 (2005) 132402.

6 Zhou J P, Dass R, Yin H Q, Zhou J S, Rabenberg L & Goodenough J B, *J Appl Phys*, 87 (2000) 5037.

7 Sarma D D, Mahadeva P, Saha-Dasgupta T, Ray S & Kumar A, *Phys Rev Lett*, 85 (2000) 2549.

8 Asano H, Kozuka N, Tsuzuki A & Matsui M, *Appl Phys Lett*, 85 (2004) 263.

9 Kahoul A, Azizi A, Colis S, Stoeffler D, Moubah R, Schmerber G, Leuvrey C & Dinia A, *J Appl Phys*, 104 (2008) 1.

10 Li Q F, Wang L & Su J L, *Mod Phys Lett B*, 25 (2011) 2259.

11 Aloysius R P, Pandey V, Verma V, Awana V P S, Kotnala R K & Kothari P C, *Sens Lett*, 7 (2009) 224.

12 Pandey V, Verma V, Aloysius R P, Bhalla G L, Awana V P S, Kishan H & Kotnala R K, *J Magn Magn Mater*, 321 (2009) 2239.

13 Savrasov S Y & Savrasov D Y, *Phys Rev B*, 46 (1992) 12181.

14 Savrasov S Y, Program LMTART for electronic structure calculations, Los Almos National Laboratory, (2004); Savrasov S Y, FULL-POTENTIAL PROGRAM PACKAGE ”LMTART 6.50” USER’s MANUAL, New Jersey Institute of Technology, (2004).

15 Perdew J P & Wang Y, *Phys Rev B*, 45 (1992) 13244.

16 M Musa Saad H E & El-Hagary M, *J Magn Magn Mater*, 360 (2014) 229.

17 Lufaso M W & Woodward P M, *Act Cryst B*, 57 (2001) 725.

18 Shannon R D, *Acta Cryst A*, 32 (1976) 751.

19 M Musa Saad H E, *Comp Mater Sci*, 82 (2014) 325.

20 Fernandez I, Greatrex R & Greenwood N N, *J Solid State Chem*, 32 (1980) 97.

21 M Musa Saad H E, *Mater Chem Phys*, 204 (2018) 350.

22 Ramesha K, Thangadurai V, Sutar D, Subramanyam S V, Subbanna G N & Gopalakrishnan J, *Mater Res Bull*, 35 (2000) 559.